Supplemental Figure 1

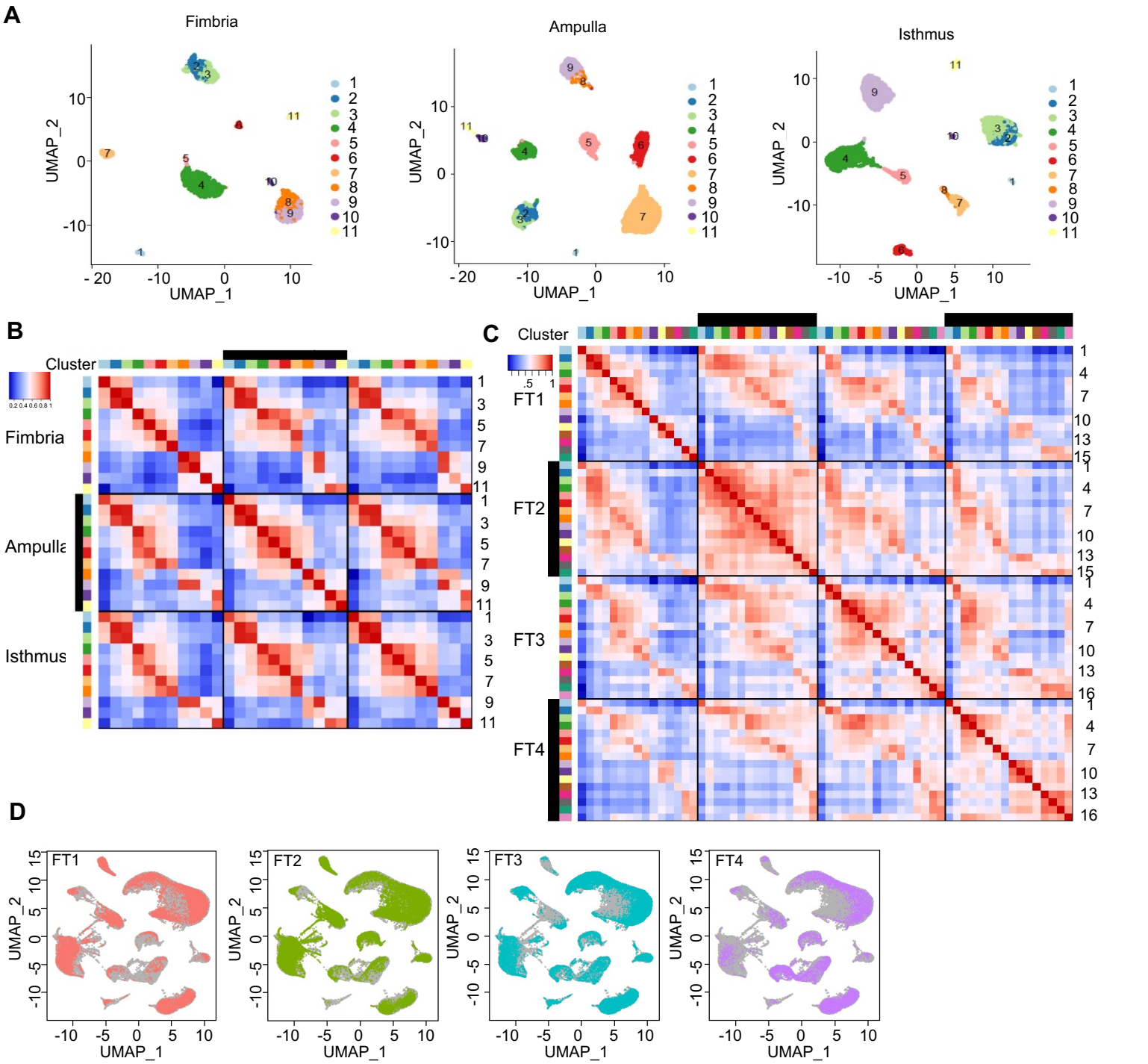

E

		1	2	3	4	5	6	7	8	9	10	11	12	Total
FT1	F	2.3%	22.7%	8.9%	24.2%	0.6%	0.9%	2.4%	5.3%	0.6%	27.5%	1.3%	3.1%	1856
	A	0.8%	13.6%	8.7%	34.1%	10.6%	7.1%	9.0%	1.1%	0.7%	11.3%	0.2%	2.7%	4901
	I	0.9%	27.7%	6.6%	18.9%	5.6%	4.2%	7.1%	1.6%	0.8%	22.9%	1.2%	2.5%	3700
FT2	F	15.6%	41.0%	4.7%	20.5%	0.4%	0.3%	2.5%	2.3%	0.0%	6.7%	3.5%	2.6%	9314
	A	4.4%	48.3%	3.0%	2.5%	12.7%	8.3%	11.6%	0.6%	0.0%	2.4%	3.4%	2.7%	8020
	I	1.1%	28.4%	6.0%	4.7%	19.6%	9.7%	20.1%	0.7%	0.1%	2.8%	4.0%	3.1%	8033
FT3	F	4.2%	16.3%	18.3%	21.4%	0.2%	0.0%	0.3%	13.6%	0.2%	14.8%	3.8%	7.0%	8152
	A	3.0%	9.2%	22.6%	19.3%	2.6%	0.6%	2.3%	11.2%	1.1%	13.2%	2.2%	12.8%	2180
	I	1.4%	5.5%	19.1%	25.4%	2.9%	0.5%	2.7%	6.7%	5.1%	18.9%	5.0%	6.7%	7022
FT4	F/A/I	4.4%	4.3%	3.5%	26.4%	0.5%	0.7%	3.0%	0.9%	0.1%	27.0%	0.7%	28.6%	6560
	Total	4.7%	23.9%	9.3%	18.4%	6.2%	3.5%	6.7%	4.0%	0.8%	12.6%	2.9%	7.0%	59738

F

ID	Assuming1% Detected %	Assuming2% Detected %
1	0.0	0.0
2	2.5	4.6
3	0.5	0.8
4	0.0	0.3
5	0.7	1.5
6	1.1	2.1
7	0.3	0.8
8	0.0	0.5
Old-13	48.6	94.3
9	0.0	0.0
10	0.0	0.1
11	0.0	0.0
12	0.4	0.4
Total	1.0	2.0

Figure S1. Assessing reproducibility of discovered cell types in healthy human fallopian tubes across tubal segments and across subjects, Related to Figure 1.

A. Consistent clustering patterns across the 3 segments from FT1. Shown are UMAP projections of the 1,861 fimbria cells, 4,944 ampulla cells, and 3,722 isthmus cells, colored by the 11 clusters independently obtained for the 3 segments.

B. Heatmap of rank correlation coefficients for pairs of cluster centroids across 11 clusters for each of the 3 segments, showing that most cell types were consistently observed across segments.

C. After combining the three segments, rank correlation coefficients of cluster centroid pairs showed consistency across fallopian tube samples from the four healthy subjects. Clustering was performed separately for each subject with cells combined across segments.

D. Visualization of the cells from each of the four samples in global UMAP projection, with one sample colored and the other three in grey.

E. Cell type composition of the 12 major cell types, compared across the 10 fallopian tube segment samples in the 4 healthy subjects.

F. Apparent doublet rates for the 12 major cell types, plus "Cluster-13" that was identified as doublets in early processing. Results were from running *DoubletFinder* for FT1 at 1% and 2% assumed global doublet rates.

Supplemental Figure 2

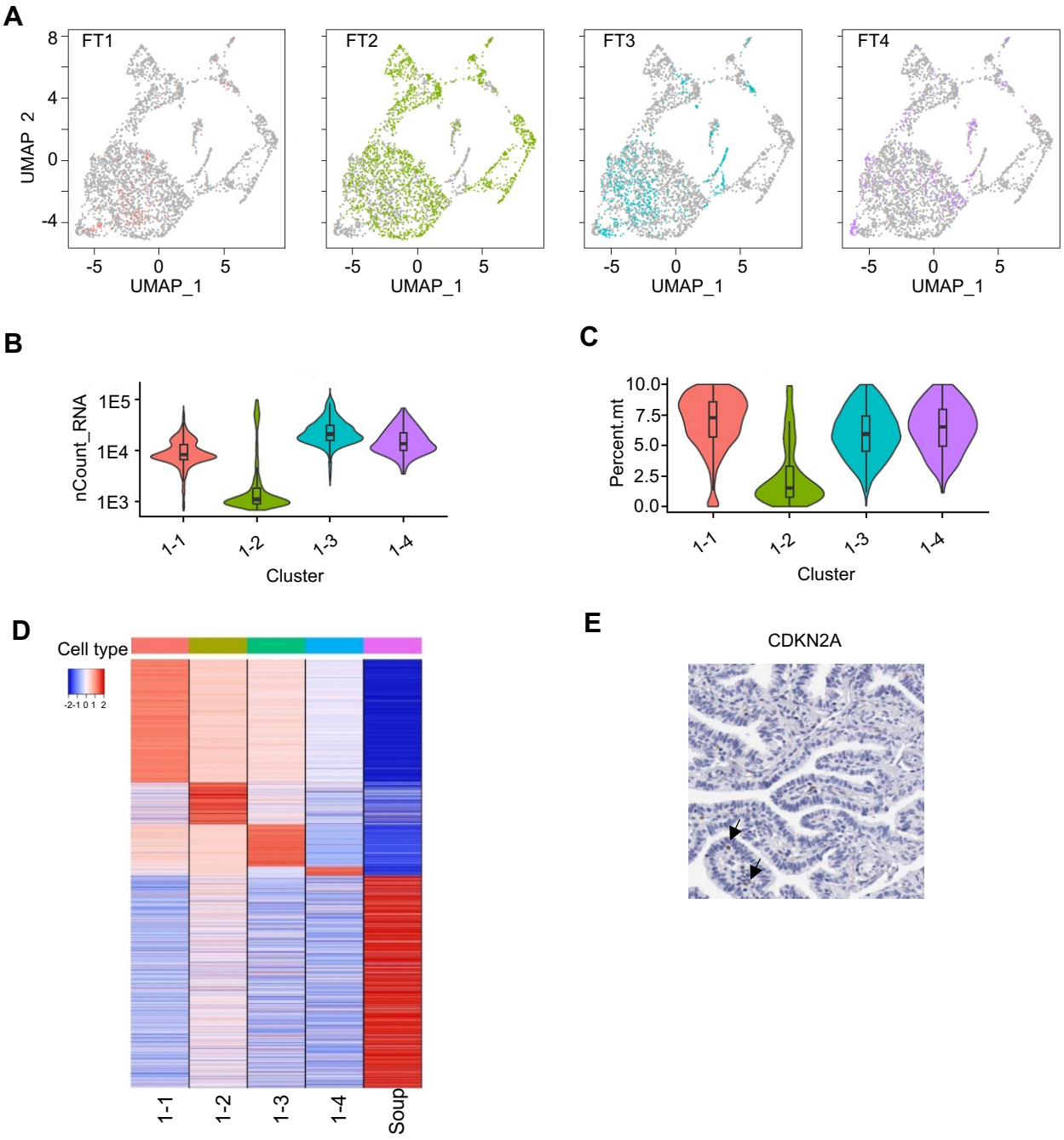

Figure S2: Ciliated cell subtypes, Related to Figure 2.

A. Consistent representation of ciliated cell subtypes in the 4 healthy fallopian tube samples. Shown are the same UMAP projection as in Fig.2A, with each panel displaying cells from one subject in color, on the grey background of cells from the other three subjects.

B. Comparison of "cell size factor", the per-cell count of detected transcripts, over the 4 subtypes.

C. Comparison of the percentage of mitochondria encoded RNA in all detected RNA for the cells.

D. Heatmap of rank correlation coefficients between individual cells (in rows) and five cluster centroids (in columns). From top to bottom are 1,452 ciliated cells of fimbria2 (ordered by their assignments into 4 subtypes) and 1,424 soup-like cells, with <100 UMIs per cell. From left to right are the correlations against the 4 CE subtype centroids and the soup centroid (see Methods). Correlation values were calculated by using 2000 highly variable genes among the 4 CE centroids.

E. Protein expression of CDKN2A in a fallopian tube section. Arrow: $CDKN2A^{+}$ cells. Image credit: Human Protein Atlas, www.proteinatlas.org (Uhlén et al., 2015). https://v21.proteinatlas.org/ENSG00000147889-CDKN2A/tissue/fallopian+tube#img

Supplemental Figure 3

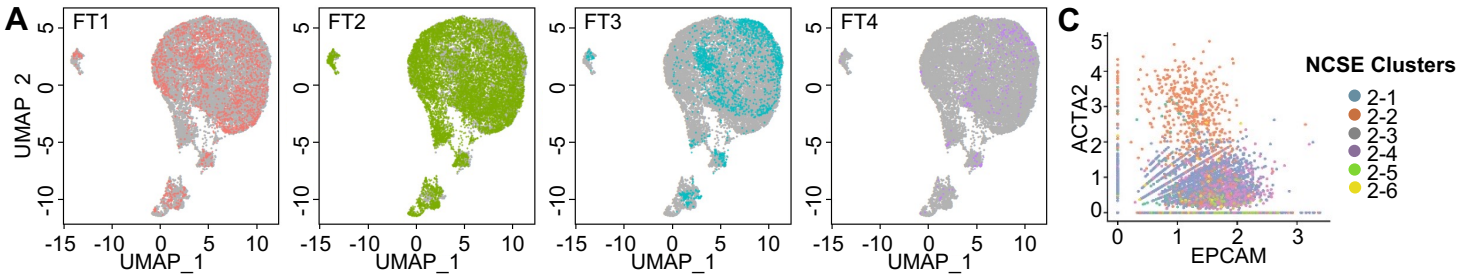

B

Cluster	2-1	2-2	2-3	2-4	2-5	2-6	Total
FT1	34 (1.6)	121 (5.7)	935 (44.2)	932 (44.1)	44 (2.1)	47 (2.2)	2113
FT2	200 (2.0)	605 (6.1)	5011 (50.2)	3942 (39.5)	21 (0.2)	194 (1.9)	9973
FT3	34 (1.8)	142 (7.4)	576 (30.1)	605 (31.6)	484 (25.3)	75 (3.9)	1916
FT4	2 (0.7)	13 (4.6)	190 (67.1)	4 (1.4)	55 (19.4)	19 (6.7)	283

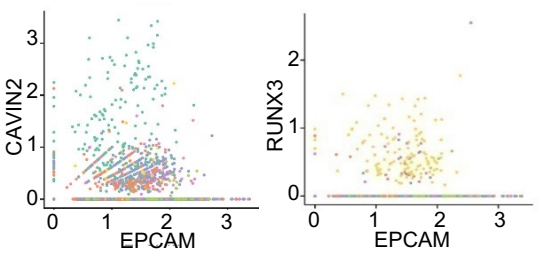

D

ID	Doublet n	Doublet %
2_1	73	27.2%
2_2	180	20.7%
2_3	0	0.0%
2_4	0	0.0%
2_5	0	0.0%
2_6	68	21.5%
Total	321	2.3%

E

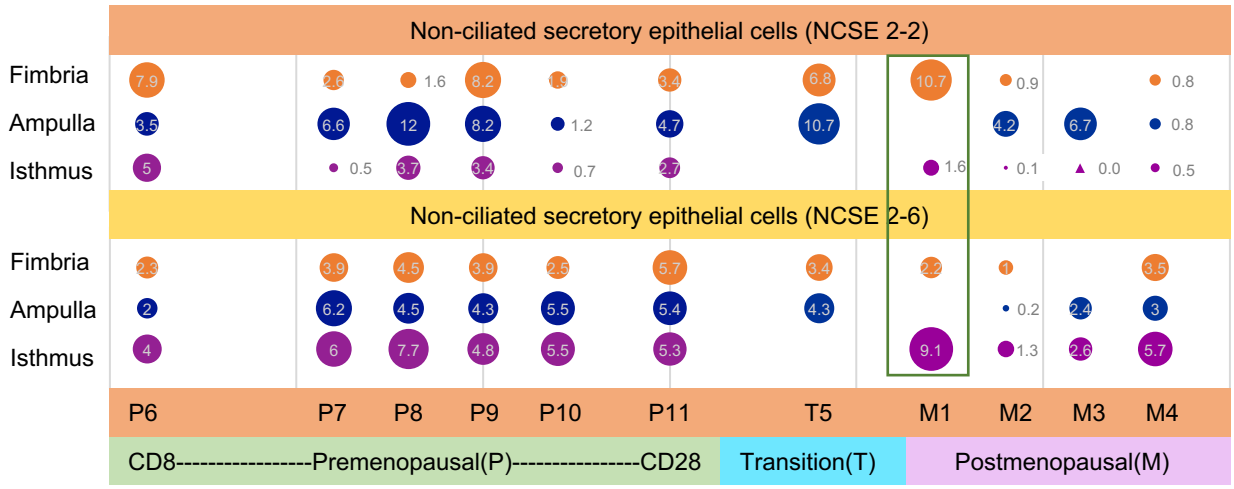

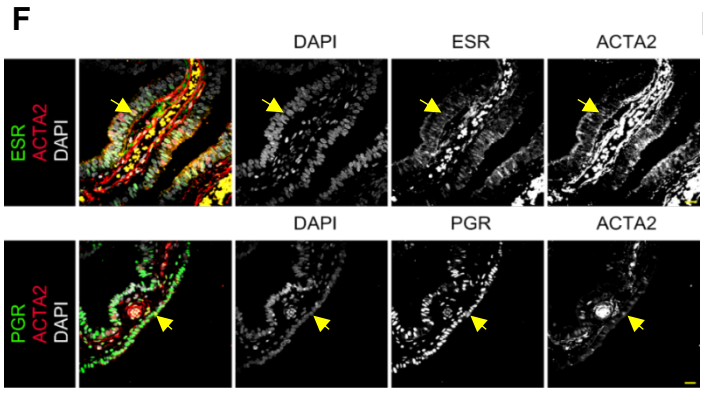

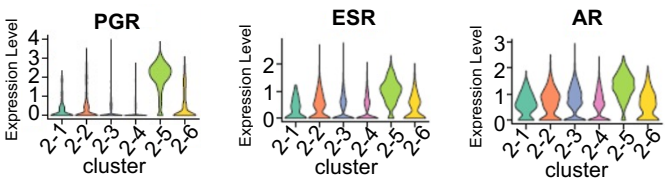

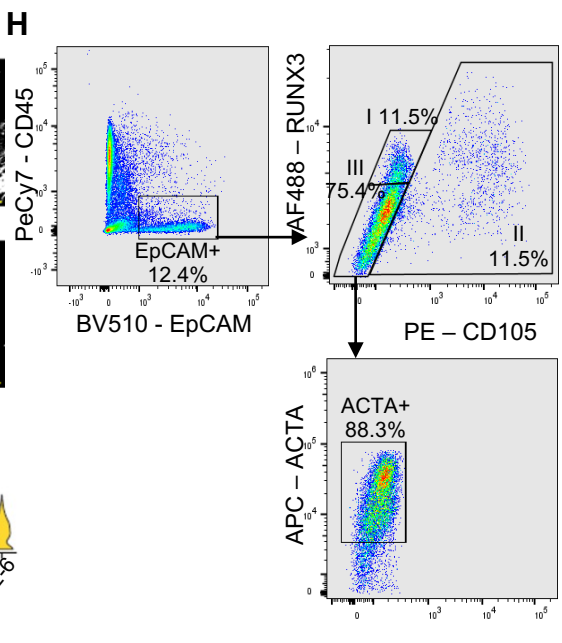

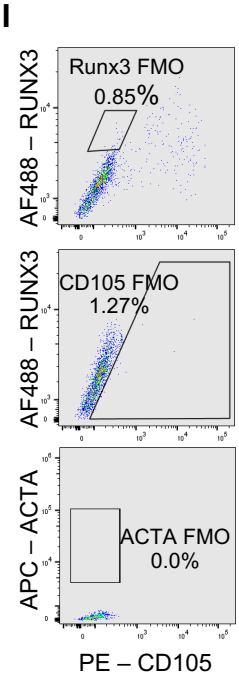

Figure S3: Secretory cell subtypes, Related to Figure 3.

A. Reproducibility of epithelial cell subtypes in the 4 healthy fallopian tube samples. Shown are the same UMAP projection as in Fig.3A, with each panel displaying cells from one subject in color, on the grey background of cells from the other three subjects.

B. Cell number and percentage of the 6 NCSE subtypes, for each of the 4 fallopian tube samples from healthy subjects.

C. Joint distribution of expression levels for 3 pairs of genes over individual cells, colored by the 6 NCSE subtypes.

D. Doublet counts and rates for the 6 NCSE subtypes in healthy FT1-3 identified by *DoubletFinder*. *DoubletFinder* analysis was performed in each of the three samples assuming 1% global doublet rate.

E. Comparison of the percentage of NCSE 2-2 cells (top), and NCSE 2-6 cells (bottom), in the 3 segments of the fallopian tube, for 11 subjects (left to right), covering different menopausal stages (indicated by P=premenopausal, T=transition, M=postmenopausal). Each subject is indicated by a number and their menopausal stage P, T, or M as described above. The post-menopausal patient using vaginal estrogen therapy is indicated by the box. NCSE2-2 and NCSE2-6 cells were by defined using a combination of $EPCAM^{+}/ACTA2^{+}/FOXJ1^{-}$ and $EPCAM^{+}$ $/RUNX3^{+}/$ $CD44^{+}$, respectively. Percent values were calculated per 1000 cells counted randomly in four quadrants of the tissue cross-section.

F. IF co-staining of ACTA2 in the fallopian tube epithelium with estrogen receptor (top) or progesterone receptor (bottom).

G. Expression levels of genes encoding hormone receptors in the 6 NCSE subtypes.

H,I. Independent validation of the molecular heterogeneity of EpCAM+ cell populations. G, Gating strategy to select EPCAM+CD45- cells. EpCAM+ cells were further stratified based on Runx3 (I), CD105 (II), double negative for both Runx3 and CD105 (III), or ACTA2 protein expression. H. Relevant flow minus one (FMO) isotype controls for each population.

Supplemental Figure 4

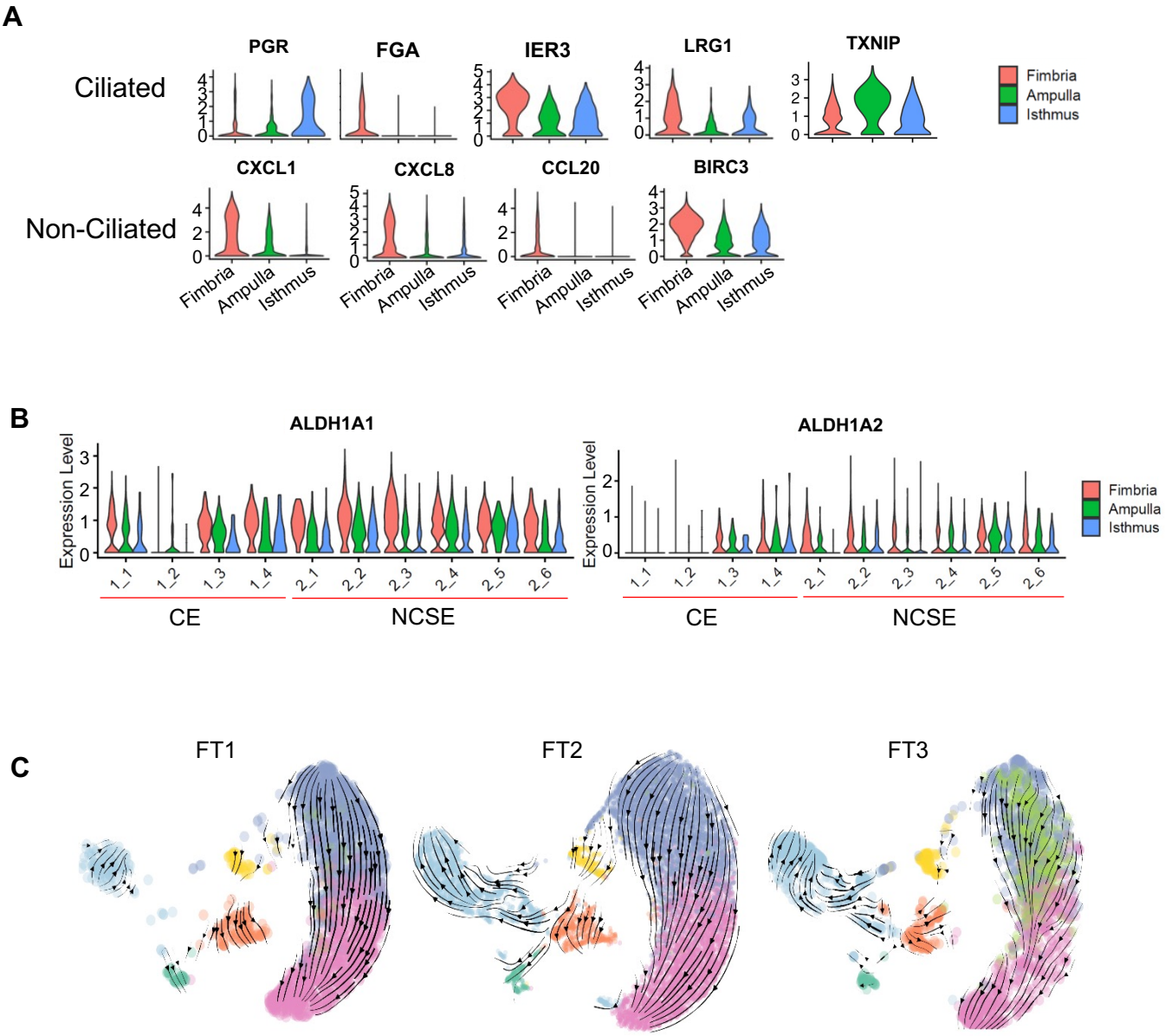

Figure S4: Gene expression differences across segments and separate velocity analysis, Related to Figure 2, 3 and 5.

A. Expression level distribution of select markers differentially expressed across the 3 tubal segments, for ciliated cells (top) and non-ciliated secretory epithelial cells (bottom).

B. Expression level distribution of ALDH1A1 and ALDH1A2 across 3 tubal segments, compared across the 4 ciliated and 6 non-ciliated secretory epithelial cell subtypes.

C. Velocity analysis for FT1-FT3 separately, revealing similar patterns as when they were analyzed together (shown in Fig 5A). UMAP coordinates were obtained by running the three samples together to ensure consistent projection of the cells when they underwent Velocity analysis for the 3 samples separately.

Supplemental Figure 5

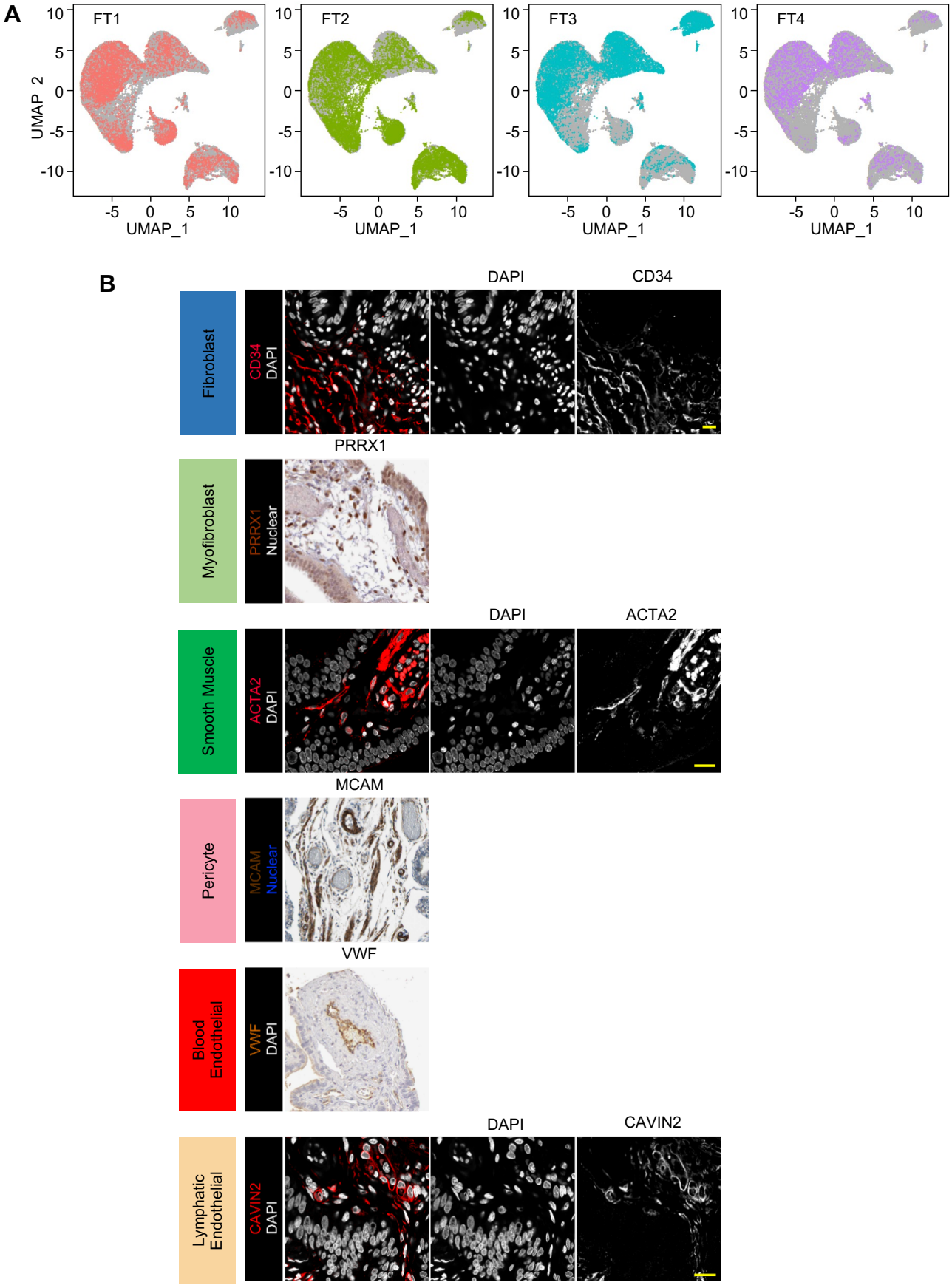

Figure S5: Stromal cells subset analysis, Related to Figure 4.

A. Consistent representation of the six stromal cell subtypes in the 4 healthy fallopian tube samples. Shown are the same UMAP projection as in Fig.4A, with each panel displaying cells from one subject in color, on the grey background of cells from the other three subjects.

B. IF staining in the fallopian tube epithelium using the antibodies against a specific marker for each of the 6 stromal cell types. PRXX1, NCAM, and VWF are courtesy of Human Protein Atlas, www.proteinatlas.org (Uhlén et al., 2015). PRXX1: https://v21.proteinatlas.org/ENSG00000116132-PRRX1/tissue/fallopian+tube#. MCAM: https://v21.proteinatlas.org/ENSG00000076706-MCAM/tissue/fallopian+tube#img. VWR: https://v21.proteinatlas.org/ENSG00000110799-VWF/tissue/fallopian+tube#img.

Supplemental Figure 6

A

Fraction of MKI67 positive cells

		Healthy 1-4 (%)	Disease 1-2 (%)
Ciliated Cells	1_1	0.06	0.35
	1_2	2.57	9.09
	1_3	0.57	1.82
	1_4	0.00	1.59
NCE Cells	2_1	0.00	8.45
	2_2	0.79	5.32
	2_3	0.54	5.55
	2_4	0.22	3.57
	2_5	1.66	4.55
	2_6	1.79	2.44
Fib		0.23	0.11
MyoFib		0.04	0.10
SM		0.00	0.22
Pericyte		0.05	0.00
B- Endo		0.03	1.08
L- Endo		0.25	0.21

B

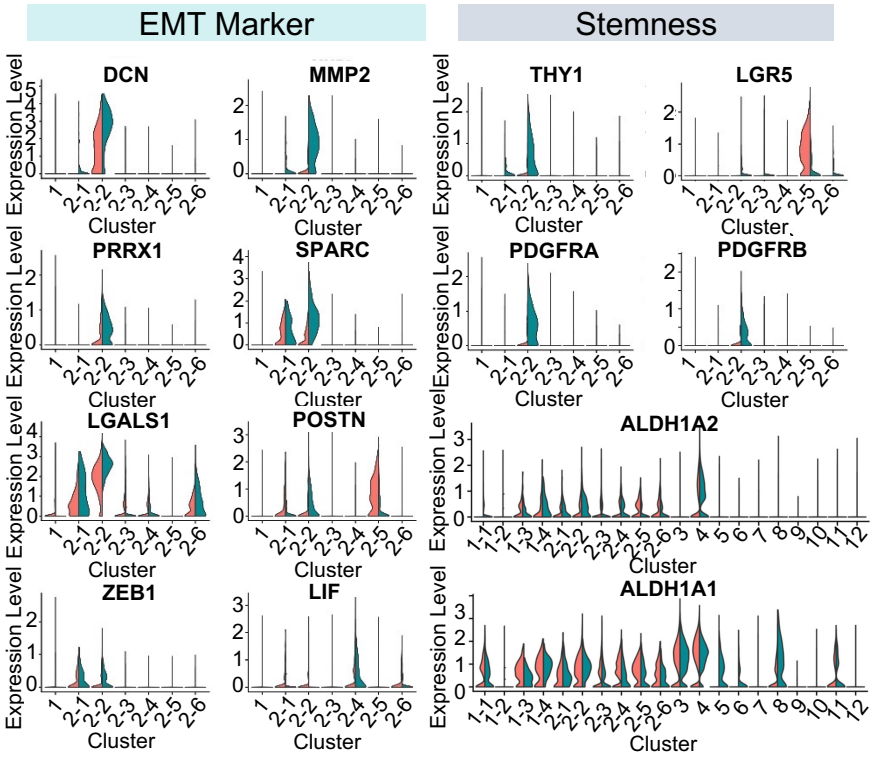

C

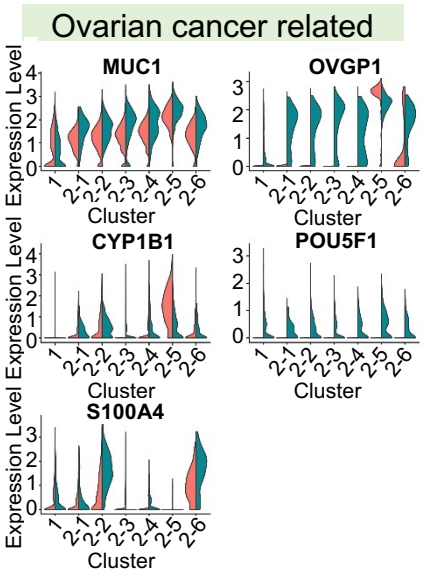

D

	1-1	1-2	1-3	1-4	2-1	2-2	2-3	2-4	2-5	2-6	Total
Number of cells											
Disease 1-2	573	11	55	63	71	301	1495	224	418	205	3416
Healthy 1-4	1724	389	525	160	270	881	6712	5483	604	335	17083
Total	2297	400	580	223	341	1182	8207	5707	1022	540	20499
% Cells											
Disease 1-2	16.8%	0.3%	1.6%	1.8%	2.1%	8.8%	43.8%	6.6%	12.2%	6.0%	1
Healthy 1-4	10.1%	2.3%	3.1%	0.9%	1.6%	5.2%	39.3%	32.1%	3.5%	2.0%	1

Figure S6: Comparison between hydrosalpinx samples and healthy fallopian tube samples, Related to Figure 6.

A. Comparison of the percentage of MKI67^{+} cells, based on transcript detection in scRNAseq data, between 4 healthy and 2 diseased samples, for 4 CE subtypes, 6 NCSE subtypes and 6 stromal cell types.

B. Expression level distribution of EMT (left) and stemness (right) markers, compared between healthy (orange) and disease (blue) samples, for CE cells, NCSE subtypes and (for ALDH1A1) the stromal cell types.

C. Expression level distribution of ovarian cancer-related genes compared between healthy (orange) and disease (blue) samples, for the CE cells and NCSE subtypes.

D. Cell number and percentage of the 4 CE subtypes and 6 NCSE subtypes, compared between the 4 healthy subjects and the 2 disease subjects.

Supplemental Figure 7

A

	1_1	1_2	1_3	1_4	2_1	2_2	2_3	2_4	2_5	2_6
X2_Ciliated_Epithelials	0.95	0.88	0.83	0.85	0.52	0.49	0.56	0.58	0.55	0.48
X1_Ciliated_Epithelials	0.91	0.85	0.78	0.81	0.44	0.41	0.48	0.49	0.47	0.43
X4_Ciliated_Epithelials	0.92	0.85	0.78	0.81	0.43	0.4	0.48	0.49	0.48	0.39
X3_Ciliated_Epithelials	0.83	0.79	0.73	0.78	0.43	0.41	0.46	0.47	0.43	0.46
Early_Secretory	0.7	0.73	0.73	0.87	0.69	0.75	0.66	0.66	0.62	0.59
X2_Secretory_Epithelials	0.69	0.74	0.84	0.74	0.86	0.85	0.89	0.89	0.9	0.86
X1_Secretory_Epithelials	0.68	0.73	0.81	0.72	0.8	0.77	0.82	0.82	0.81	0.84
X3_Secretory_Epithelials	0.65	0.71	0.83	0.71	0.88	0.87	0.9	0.92	0.89	0.89
X1_Transitional_Epithelials	0.64	0.62	0.6	0.6	0.42	0.38	0.43	0.43	0.41	0.58
X2_Transitional_Epithelials	0.28	0.36	0.42	0.33	0.57	0.53	0.57	0.55	0.54	0.73

B

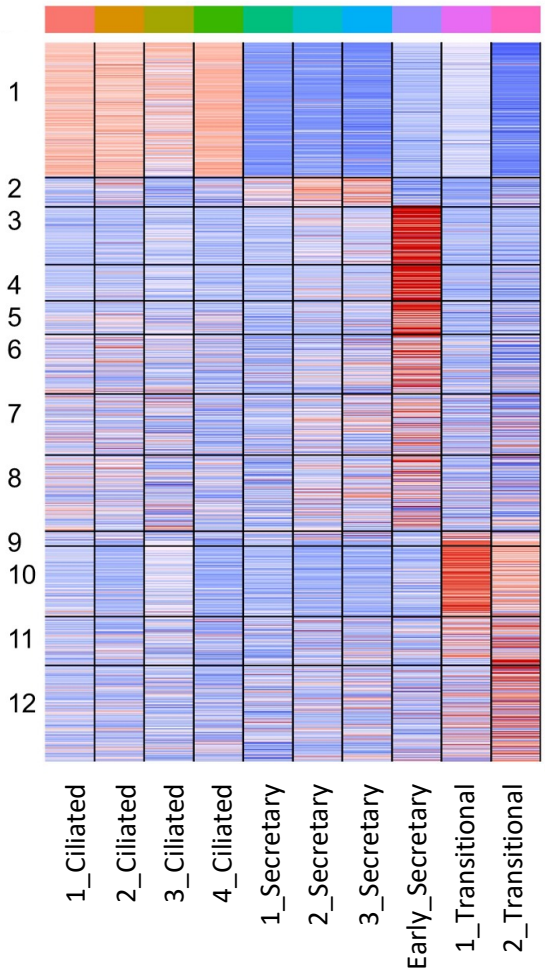

C

	Ciliated	C3	C4	C7	C9
	Ciliated	Diff	KRT17	EMT	Cycle
1_1	0.83	0.07	0.00	-0.06	-0.19
1_2	0.59	-0.13	-0.12	-0.06	-0.26
1_3	0.71	0.13	0.02	-0.07	-0.16
1_4	0.35	-0.19	-0.18	0.28	-0.58
2_1	-0.13	0.42	0.44	0.75	0.08
2_2	-0.27	0.25	0.34	0.82	-0.07
2_3	0.00	0.54	0.55	0.44	0.36
2_4	0.19	0.57	0.67	0.27	0.28
2_5	0.15	0.55	0.68	0.31	0.40
2_6	0.01	0.53	0.60	0.41	0.34

Figure S7: Comparison of cell type centroids in this study with those in Dinh et al. 2021 and Hu et al. 2020, Related to Figure 7.

A. Rank correlation coefficients between each of our ciliated and non-ciliated subtypes with each of the 10 cell types reported in Dinh et al., using 1,442 of their 1,467 markers that are also detected in our data. It showed that Dinh et al.'s ciliated cells and secretary cells are broadly consistent with ours, yet the identity of the Transitional cells are unclear, and are not in a state between our CE (1-1 to 1-4) and NCSE (2-1 to 2-6) cells.

B. Gene expression heatmap of the 10 cell type centroids reported in Dinh et al., for the 12 sets of marker genes for our 12 major cell types. The heatmap of our 12 cell type centroids was shown in Figure 1C. Marker genes for our clusters 1 and 2 are highly expressed in Dinh et al.'s Ciliated and Secretary cells, respectively. However, Early_Secretary cells express markers for our clusters 3 (fibroblasts) and 4 (myofibroblasts), while Transitional cells express markers for clusters 10 (T cells and NK cells) and 11-12 (Mast cells and macrophage).

C. Rank correlation coefficients between each of our CE and NCSE subtypes with each of the 5 clusters reported in Hu et al 2020, which included Differentiated subtype (C3), KRT17 subtype (C4), EMT (C7), Cell-cycle cluster (C9), and Ciliated. Correlations are calculated by using 51 of the 52 markers in Hu et al. that are detected in our data. It confirmed that ciliated cells in our study had the highest correlation with Hu’s Ciliated cell type, and our secretory cells had the highest correlations with Hu’s C3, C4, C7 and C9.